

Structure Study of Binary Titanophosphate Glasses Prepared by Sol-Gel and Melting Methods

Anjiang TANG, Tadanori HASHIMOTO, Tetsuya NISHIDA, Hiroyuki NASU and Kanichi KAMIYA

Department of Chemistry for Materials, Faculty of Engineering, Mie University, 1515, Kamihama-cho, Tsu-shi, Mie 514-8507

ゾル-ゲル法と溶融法で作製した二成分系チタンノリン酸塩ガラスの構造研究

唐 安江・橋本忠範・西田哲也・那須弘行・神谷寛一

三重大学工学部分子素材工学科, 514-8507 三重県津市上浜町 1515

The 70TiO₂·30P₂O₅ (mol%) glass was prepared by the sol-gel method. Its structure was examined by means of IR, Raman spectroscopy and X-ray radial distribution function analysis, and was compared with the corresponding melt-derived glass. It was found that average coordination number of Ti⁴⁺ ions was almost 6 and Ti⁴⁺ ions formed predominantly TiO₆ octahedra in the sol-gel-derived glass, while Ti⁴⁺ ions were present in the 4, 5 and/or 6-fold coordination states to give average coordination number in-between 4 and 5 in the melt-glass. The preference of high coordination state of Ti⁴⁺ ions in the sol-gel glass was consistent with higher refractive index and density than the melt-glass.

[Received May 17, 2004; Accepted July 30, 2004]

Key-words : Sol-gel method, TiO₂-P₂O₅ glass, FT-IR, Raman, Coordination number, Atomic radial distribution function

1. Introduction

Titania has been one of important constituent oxides of glasses to tailor linear and non-linear optical properties, because of its high polarizability or molar refraction. From the view point of the ecology, titania has been believed to be an excellent light-weight substitute for toxic heavy metals such as Pb in commercial optical glasses. However, the solubility of titania in the silica, for example, is not high enough to attain the refractive index as high as 2.0. It has been known that only P₂O₅ can dissolve TiO₂ up to about 70 mol% to form the TiO₂-P₂O₅ glasses. So far, the glasses have been prepared using several authors by the conventional melting method.^{1)–3)} Those glasses are known to show the electronic conduction due to the coexistence of Ti³⁺ ions with Ti⁴⁺ ions, but are colored in dark purple by Ti³⁺ ions present. Therefore, scarce attention has been paid to those glasses in optical applications.

We have succeeded in making highly transparent, colorless and high-index TiO₂-P₂O₅ glasses containing TiO₂ up to 74 mol% by re-heat-treating the “black” glasses around their glass transition temperatures in the air for a long time.⁴⁾ Then, they are now expected to be applicable to photonic devices such as ultrafast optical switches and optical limiters.

Recently, we also reported the preparation of bulk glasses in the TiO₂-P₂O₅ system containing TiO₂ up to 95 mol% by the sol-gel method using titanium and phosphorus alkoxides as starting materials.⁵⁾ The refractive index of the sol-gel-derived x TiO₂·(100- x)P₂O₅ (mol%) glass was 2.099 at $x=70$ which was higher than that (1.919) of the corresponding melt-derived glass, and was increased with x to reach ~2.3 at $x=90$ –95. On the other hand, the density of the sol-gel glass was higher than the melt-glass at $x=70$. Such a difference in the property between glasses prepared by two different methods was supposed to arise from the difference in structure, especially in the coordination state of Ti⁴⁺ ions.

In the present work, the structure of the 70TiO₂·30P₂O₅ (mol%) glasses prepared by the sol-gel method and melting method was examined by means of FT-IR, Raman spectroscopy and also X-ray radial distribution function analysis,

and was discussed with focusing on the coordination state of Ti⁴⁺ ions.

2. Experimental

2.1 Preparation of glass samples

In the sol-gel preparation, reagent grade titanium tetraisopropoxide, Ti(O-*i*-C₃H₇)₄ (TIP, Wako Pure Chemicals Co.) and triethyl phosphate PO(OC₂H₅)₃ (TEP, Nacalai Tesque Inc.) were used as raw materials. The guaranteed 2-methoxyethanol (Nacalai Tesque Inc.) was used as a solvent, and HCl as a catalyst. First, TIP was mixed with TEP to give the oxide composition of 70TiO₂·30P₂O₅ in mol%. After 1 h-stirring, the alkoxide mixture was diluted with 2-methoxyethanol. Then after another 1h, the solution consisting of water, HCl and 2-methoxyethanol was added dropwise using a burette while stirred and cooled in the water/ice bath. The composition of the resultant solution is given in Table 1 in molar ratios.

The sol thus prepared was poured into a loosely covered container made of polypropylene and kept standing in the room until it set to a gel. The wet gel was transferred to a 60°C-oven and held there for three weeks to dryness, and heat-treated up to 500, 550 or 600°C in the air with a heating rate of 3°C/min.

The glass having the composition of 70TiO₂·30P₂O₅ (mol%) was also prepared from the corresponding mixture of reagent grade TiO₂ (Kojundo Chemical Laboratory Co.,

Table 1. Composition of the Starting Solution for the 70TiO₂·30P₂O₅ (mol%) Glass (in Molar Ratios)

TIP	TEP	H ₂ O	2-methoxyethanol	HCl
1	0.86	8	25	0.05

TIP: Ti(O-*i*-C₃H₇)₄, TEP: PO(OC₂H₅)₃

Ltd.) and $\text{NH}_4\text{H}_2\text{PO}_4$ (Nacalai Tesque Inc.) by the melting method. For that, the mixture was placed in an alumina crucible and heated at 1000°C for 1 h to degas NH_3 from $\text{NH}_4\text{H}_2\text{PO}_4$, followed by melting at 1300°C for 5 h under the air atmosphere. The melt was poured onto an iron plate preheated to 100°C and quenched by pressing with another iron plate. The "black" glass thus obtained was re-heat-treated at 650°C for 48 h to oxidize included Ti^{3+} ions which were responsible for dark purple color of the glass.

2.2 Structure measurements and analyses

Conventional continuous X-ray diffraction measurements were made to confirm the amorphous state of the sol-gel samples and to identify the crystalline species occasionally precipitated, by using Shimadzu XD-610 X-ray diffractometer. The Ni-filtered $\text{Cu K}\alpha$ radiation was used as an X-ray source.

Fourier-transform infrared (FT-IR) spectra were obtained by the KBr pellet method in the wavenumber range of 400 to 1200 cm^{-1} with a resolution of 1 cm^{-1} . Fourier-transform IR spectrophotometer FT/IR-550 (JASCO Co.) was used.

Raman spectra were measured using a laser Raman spectrometer Ramanor T64000M1 (Atago Bussan Co., Ltd.). The 514.5 nm emission line of an argon ion laser was used for excitation with an incident power of 100 mW . Accumulation times 10 and Raman shift range of 200 to 1500 cm^{-1} were selected as measurement conditions.

X-ray measurements for atomic radial distribution function analysis of the glasses were preformed by using a machine Geiger Flex RAD (Rigaku Co., Ltd.). The $\text{Cu K}\alpha$ and $\text{Mo K}\alpha$ radiations monochromatized by balanced filters and a graphite monochromator were used as X-ray sources. The X-ray scattering intensity was measured at a diffraction angle (θ) interval of $2\theta=0.5^\circ$ by a scintillation counter equipped with a pulse-height analyzer. At least, 10,000 counts were accumulated at each angle. The scattering measurement range was 0 to 150 nm^{-1} in $S=4\pi\sin\theta/\lambda$ (λ : wavelength of X-ray).

After correcting the scattering intensity for polarization, absorption and background due to air scattering, two intensity curves obtained by using $\text{Cu K}\alpha$ and $\text{Mo K}\alpha$ radiations were combined to form single scattering intensity curve, and normalized to electron units by a method combining Krogh-Moe and Norman's⁶⁾ method with the high angle method. The normalized X-ray scattering intensity was Fourier-transformed into the atomic radial distribution function (RDF) according to Eq. (1).

$$\text{RDF}(r) = \sum K_m 4\pi r^2 \rho_0 + \frac{2r}{\pi} \int_0^{S_{\max}} S \cdot i(S) \times \exp(-\alpha^2 S^2) \sin(r \cdot S) dS \quad (1)$$

where $S=4\pi\sin\theta/\lambda$, K_m is the effective number of electrons in the glass sample, r the interatomic distance and $\exp(-\alpha^2 S^2)$ a damping factor, and ρ_0 an average electron density of the glass sample.

In order to determine the interatomic distance and coordination number of cations with respect to oxygens, the deconvolution of first peak in RDF curve by the least-square fitting with Gaussian function was performed. The coordination number, n of Ti^{4+} or P^{5+} ions with respect to oxide ions was estimated from the area (AP) under the deconvoluted peak for Ti-O or P-O pairs using a following Eq. (2).

$$\text{AP} = 2 \times a \times K_{\text{Ti}} (\text{or } K_{\text{P}}) \times K_{\text{O}} \times n \quad (2)$$

where a is the molar content of TiO_2 (or $\text{PO}_{5/2}$) in the unit composition used to calculate RDF, effective electron num-

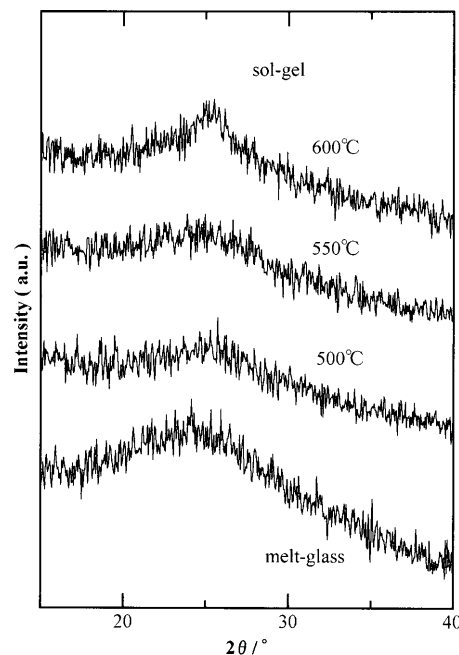


Fig. 1. X-ray diffraction patterns of gel samples heat-treated at 500, 550 and 600°C , and melt-derived glass of the $70\text{TiO}_2 \cdot 30\text{P}_2\text{O}_5$ (mol%) composition.

bers K_{Ti} , K_{P} and K_{O} are 25.2, 16.3 and 6.97, respectively, in the present case.

3. Results

Samples obtained by heat-treating the gels to 500 – 600°C , and the melt-glass were colorless and transparent, indicating that they are free from Ti^{3+} ions.

Figure 1 shows conventional X-ray diffraction (XRD) patterns of the sol-gel-samples heat-treated to 500 , 550 and 600°C , and that of the melt-glass. While a faint diffraction peak corresponding to precipitated anatase by a few mass% is observed around $2\theta=25^\circ$ for the 600°C -treated sample, the 500 and 550°C -treated samples are seen to be amorphous. So, the sol-gel samples heat-treated to 500 and 550°C are "glass" (as was reported, corresponding bulk samples exhibited the "glass-transition" phenomenon). In addition, the film specimen deposited on an Si wafer and heat-treated showed no discernible IR peak around 3500 cm^{-1} , indicating that the glass sample does not contain a detectable amount of the OH groups.

FT-IR spectra of sol-gel glasses, partially crystallized sol-gel glass and the melt-glass are shown in **Fig. 2**. A strong absorption peak observed at 1000 – 1100 cm^{-1} for all the samples is one that has been assigned to the stretching vibration of P-O bonds in $\text{O}=\text{PO}_3$ tetrahedra (for simplicity, hereafter described as PO_4) and in those associated with other cation-oxygen polyhedra (in the present case, P-O-Ti). IR absorption peaks (or humps) around 800 and 610 cm^{-1} are attributable to Ti-O stretching vibration as will be discussed in the next section.

Any remarkable difference in whole spectrum feature and the absorption peak position between sol-gel glasses and the melt-glass is not noted.

Raman spectra of the present glasses are shown in **Fig. 3**. Peaks are observed at Raman shifts of 1000 – 1100 , 810 , 630 , 510 , 400 and $\sim 290\text{ cm}^{-1}$ in all the glasses as reported by Brow et al.³⁾ for the "black" glass. As to the melt-derived glass, the

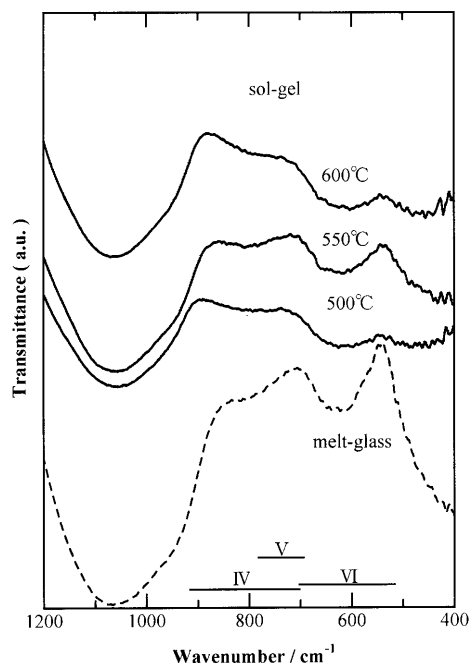


Fig. 2. FT-IR spectra of sol-gel-derived glasses and melt-derived glass.

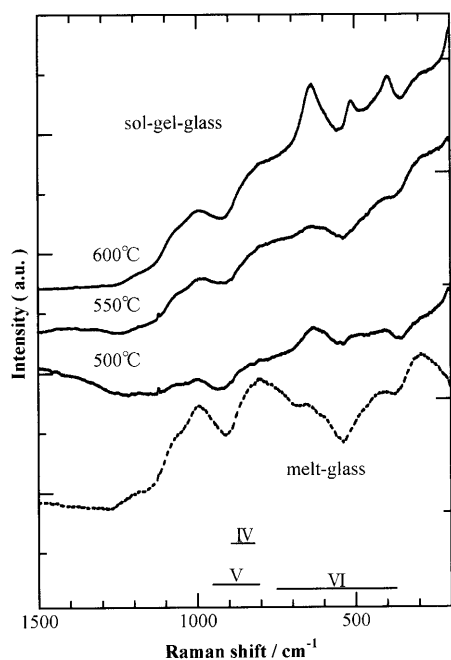


Fig. 3. Raman spectra of sol-gel-derived glasses and melt-derived glass.

alumina of several mol% may be contained as the contaminant from the alumina crucible used for melting, as has been reported by Brow et al.³⁾ However, any peaks other than those associated with Ti, P and O atoms were not detected in IR and Raman spectra.

A peak at 1000–1100 cm^{-1} is assigned to P–O bonds, and other peaks below 900 cm^{-1} except one at $\sim 290 \text{ cm}^{-1}$ are related to Ti–O bonds in the glasses. As is seen from the spectrum of partially crystallized glass (600°C-treated sample), peaks at 610, 530 and 400 cm^{-1} are attributed to Ti–O bonds

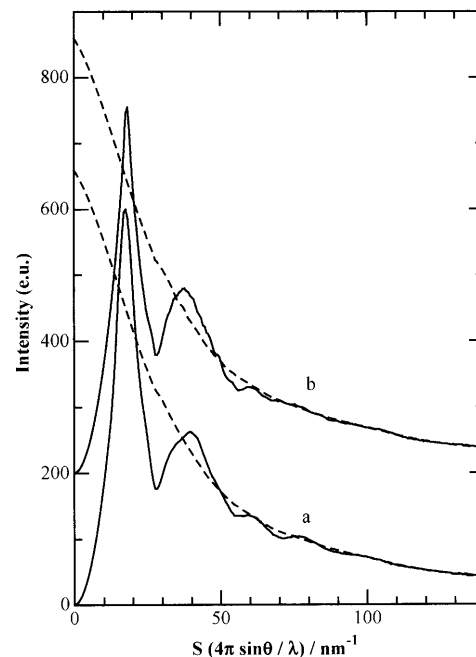


Fig. 4. X-ray scattering intensity curves of the 70TiO₂·30P₂O₅ glasses (a) the melt-derived glass and (b) the sol-gel-derived glass. The broken line stands for the theoretical scattering curve.

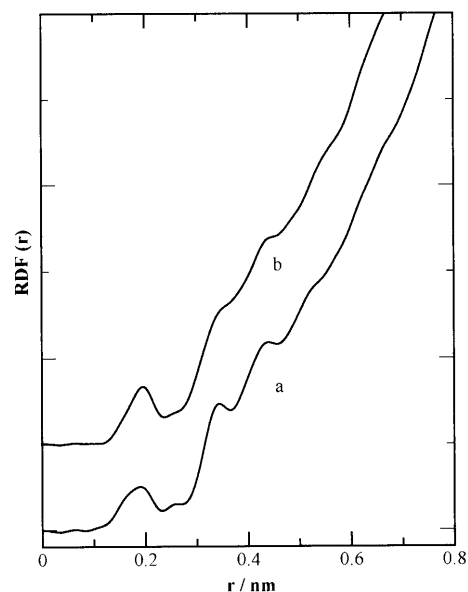


Fig. 5. Radial distribution function curves of the 70TiO₂·30P₂O₅ glasses (a) the melt-derived glass and (b) the sol-gel-derived glass.

in crystalline TiO₂ (anatase). The peak around 800 cm^{-1} is prominent in the melt-glass, while it is small in the sol-gel glasses compared to peaks in the Raman shift range of 400 to 600 cm^{-1} . The Raman peak assignment and the difference of the spectrum between the glasses will be discussed in the following section, with relation to the coordination state of Ti⁴⁺ ions.

X-ray scattering intensity curves of the 70TiO₂·30P₂O₅ glass obtained by heat-treating the gel at 550°C, and the corresponding melt-glass are shown in Fig. 4. Figure 5 shows RDF curves of those glasses. In the calculation of X-ray struc-

ture parameters of the melt-derived glass, the nominal composition was used for simplicity. This is because the X-ray scattering factor of the contaminant Al^{3+} is close to P^{5+} , and the number of Al-O pairs is considered so small that the pairs may not contribute to the first RDF peak to the extent larger than the experimental error.

Several peaks or humps can be observed in respective RDF curves shown in Fig. 5. Considering the interatomic distance and glass composition, a relatively strong first peak observed at 0.15 to 0.2 nm should be a composite peak due to the nearest P-O and Ti-O pair correlations. The deconvolution results of the first peak into two component peaks are shown in Figs. 6(a) and (b) for the melt-glass and sol-gel-glass, respectively. Since the interatomic distance 0.155 or 0.156 nm is almost identical with the P-O distance found in phosphate glasses and/or crystalline phosphates so far reported,⁷⁾ another component peak at 0.194 or 0.197 nm is assignable to the Ti-O correlation.

The coordination numbers of P^{5+} and Ti^{4+} ions with respect to oxide ions, which were evaluated from the area under respective component peaks are listed in Table 2, as well as interatomic distances. It is clearly seen that the coordination number of Ti^{4+} ions is larger in the sol-gel-glass than in the melt-glass, while the coordination number of P^{5+} ions is about 4 in both glasses.

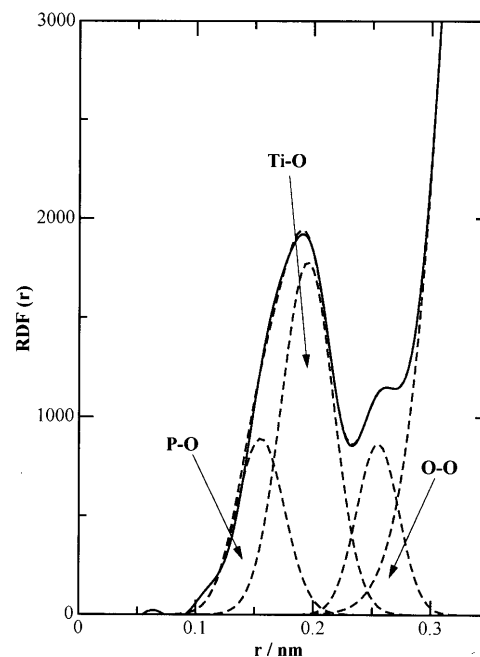
The second peak appears at 0.346 nm in the RDF curve of the sol-gel-glass, and at slightly smaller distance as 0.341 nm in the curve of the melt-glass. This may indicate some difference in the second coordination shell between the sol-gel and melt-glasses. On the other hand, any significant difference in the distance of third peak between two glasses is noted.

4. Discussion

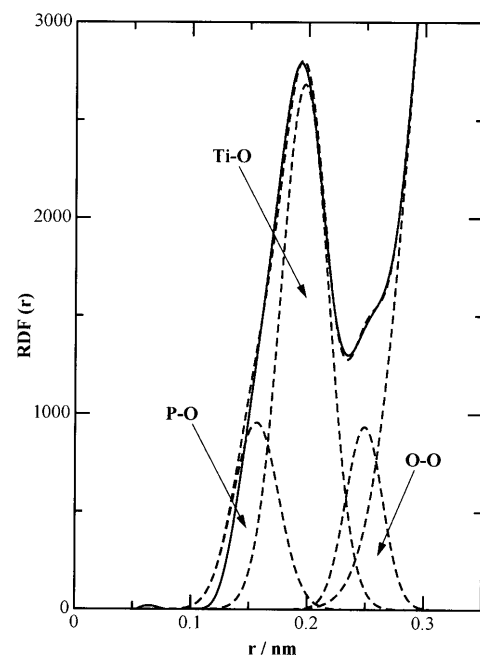
For examining and discussing the structure or especially coordination states of P^{5+} and Ti^{4+} ions in the present glasses on the basis of vibrational spectroscopy data, assignments of peaks in IR and Raman spectra of P_2O_5 and/or TiO_2 containing glasses and crystals refer to literatures and are summarized in Tables 3 and 4. The IR absorption wavenumber ranges read from Table 3 for respective coordination states of Ti^{4+} ions with respect to oxide ions are indicated by bars in Fig. 2. It is now easily understood that a relatively strong absorption peak at $\sim 610\text{ cm}^{-1}$ is from 6-fold coordinated Ti^{4+} ions, and a hump covering wavenumber range from 700 to 900 cm^{-1} is assignable to 4 or 5-fold coordinated Ti^{4+} ions. However, the difference in the coordination state of Ti^{4+} ions between the sol-gel and melt-glasses is difficult to be mentioned, because of no essential difference of IR spectrum feature.

The Raman shift ranges for Ti^{4+} ions in different coordination states, which can be read from Table 4, are also indicated by bars in Fig. 3. According to those published data, a Raman peak observed for the present glasses in the range of $750\text{--}900\text{ cm}^{-1}$ is attributable to 4 or 5-fold coordinated Ti^{4+} ions, and three peaks appearing below 700 cm^{-1} to 6-fold ones. The assignment of the latter three peaks to 6-fold coordinated Ti^{4+} ions is very reasonable because they are those found in crystalline titania (anatase).

By comparing Raman spectra of the sol-gel-glasses and melt-glass with each other, it is found that 4 or 5 fold coordinated Ti^{4+} ions are more abundant than 6-fold ones in the melt-glass, and 6-fold coordinated Ti^{4+} ions are predominant in the sol-gel-glasses. However, it seems difficult to distinguish between 4-fold coordination state of Ti^{4+} ions and 5-fold ones in the spectrum of the melt-glass. As to the chemical environment of P^{5+} ions, it is considered from IR and



(a)



(b)

Fig. 6. Peak deconvolution result for the first RDF peak of (a) the melt-derived and (b) sol-gel-derived $70\text{TiO}_2\cdot 30\text{P}_2\text{O}_5$ glasses.

Table 2. Atomic Distance and Coordination Number for P-O and Ti-O Pairs in Melt-Derived Glass and Sol-Gel-Derived Glass

Glass sample	P-O (nm)	Coordination number	Ti-O (nm)	Coordination number
Melt-derived	0.155	3.93	0.194	4.72
Sol-gel-derived	0.156	4.15	0.197	6.47

Raman spectroscopic data that there is not any essential difference between two kinds of glasses.

Structure information based on IR or Raman spectroscopy is rather qualitative. On the other hand, more quantitative information on coordination states of P^{5+} and Ti^{4+} ions, and bond lengths of P-O and Ti-O in the present glasses are obtainable from the atomic radial distribution analysis results, as listed in Table 2. Taking into consideration the experimental error and the fact that the K-approximation does not strictly hold for P-O and Ti-O pairs, the coordination number of P^{5+} ions is regarded as 4 in both glasses, and that of Ti^{4+} ions as 4-5 in melt-glass and as 6 in the sol-gel-glass, respectively.

With regard to the interatomic distance, the experimental error has been evaluated to be ± 0.001 nm. Therefore, it is mentioned that there is not any significant difference in the P-O bond length between two glasses, and the Ti-O bond length in the sol-gel-glass is slightly larger than in the melt-glass. The bond length and coordination number of P^{5+} ions are consistent with those so far published for phosphate glasses and crystals, indicating that P^{5+} ions are present with forming PO_4 tetrahedra.

It is known that the range of Ti-O distance in TiO_6 octahedra is 0.171-0.234 nm in $Na_2Ti_3O_7$,¹⁶⁾ 0.195-0.209 nm in Ti_2CaO_4 ,¹⁷⁾ 0.194-0.195 nm in $Sr_3Ti_2O_7$,¹⁸⁾ 0.191-0.195 nm in anatase, brookite and rutile.¹⁹⁾

A slightly shorter Ti-O bond length observed in the melt-derived glass, on the other hand, could be interpreted in

different manners. First, assuming that the Ti-O bond length is the result of averaging those in the mixture of TiO_4 tetrahedra (Ti-O bond length is 0.174 nm^{20),21)} and TiO_6 octahedra when the coordination number of Ti^{4+} ions is in-between 4 and 6, the Ti-O bond length of 0.194 nm may lead to the TiO_6 fraction of $\sim 90\%$ or the average coordination number of 5.8 for Ti^{4+} ions. This coordination number is much larger than experimental value.

Then, secondly, the presence of 5-fold coordinated Ti^{4+} ions forming TiO_5 pyramids is assumed in the melt-glass. The TiO_5 pyramidal units have been found in $K_2Ti_2O_5$ crystal,²²⁾ in which Ti=O bond length is 0.157 nm and that of other four Ti-O bonds is 0.200 nm. Yarker et al. found the TiO_5 pyramids in the K_2O - TiO_2 - SiO_2 glass by the neutron diffraction method, and reported that the interatomic distance is 0.163-0.167 nm for Ti=O and is 0.194-0.196 nm for Ti-O.²³⁾ The average Ti-O distance in a TiO_5 pyramid is thus 0.191 nm, which is more close to the experimental value. Accordingly, the occurrence of 5-fold coordinated Ti^{4+} ions in preference to the coexistence of 4 and 6-fold ones would be predicted in the melt-glass. However, it should be noted that the resolution power of the X-ray diffraction method is not high enough to make difference between above assumptions. Eventually, combining vibrational spectroscopy data with the RDF results, it may be more reasonable to assume the coexistence of 4, 5 and 6-fold coordinated Ti^{4+} ions in the melt-glass and the abundance of the former two relative to the last one.

A small hump appearing around 0.25 nm in RDF curve (which is clearly observed in the deconvolution results shown in Figs. 6(a) and (b)) corresponds to the shortest O-O distance in the PO_4 tetrahedra. Second prominent peak at 0.34-0.35 nm is attributable to the interpolyhedral correlation of cation pairs like the nearest intertetrahedral Si-Si correlation in the silica glass which gives rise to a RDF peak around 0.3 nm. Several cation pairs such as P-O-P, Ti-O-Ti and P-O-Ti are supposed to occur, and they, if any, should exhibit peaks around 0.32 nm (P-O-P), 0.4 nm (Ti-O-Ti for corner-shared TiO_6 or TiO_5 polyhedra), 0.28 nm (Ti-O-Ti for edge-shared TiO_6 or TiO_5 polyhedra), 0.34 nm (Ti-O-Ti for corner-shared TiO_4) and 0.34 nm (Ti-O-P for corner-shared PO_4 - TiO_x ($x=5$ or 6)). Among those atomic pairs, the Ti-O-P interpolyhedral correlation is most probable because the P/Ti atomic ratio of the glasses is 0.6/0.7, near unity.

Slightly larger distance of first P-(O)-Ti pairs in the sol-gel-glass is reasonable since PO_4 tetrahedra are bonded mostly to TiO_6 octahedra. The assignment of other peaks in the RDF curve at larger interatomic distance, and the discus-

Table 3. Assignments of IR Absorption Peaks of TiO_2 -Containing Glasses

Composition	Peak / cm^{-1}	Assignment	Reference
Ti-O stretching vibration of TiO_4 tetrahedra			
$\text{TiO}_2\text{-SiO}_2$ } $\text{TiO}_2\text{-Na}_2\text{O-SiO}_2$ }	940		8)
$\text{K}_2\text{O-TiO}_2$ } $\text{Cs}_2\text{O-TiO}_2$ }	780		9)
$\text{Na}_2\text{O-TiO}_2\text{-SiO}_2$	690-800		10)
Ti-O stretching vibration of TiO_5 square pyramid			
$\text{Na}_2\text{O-TiO}_2\text{-SiO}_2$	740		10)
Ti-O stretching vibration of TiO_6 octahedra			
$\text{K}_2\text{O-TiO}_2$ } $\text{Cs}_2\text{O-TiO}_2$ }	610, 700		9)
$\text{TiO}_2\text{-SiO}_2$ } $\text{TiO}_2\text{-Na}_2\text{O-SiO}_2$ }	570		8)
$\text{Na}_2\text{O-TiO}_2\text{-SiO}_2$	550-600		10)

Table 4. Assignments of Raman Shift of TiO_2 -Containing Glasses

Composition	Raman shift / cm ⁻¹	Assignment	Reference
		Ti-O stretching vibration of TiO ₄ tetrahedra	
<div>Li₂Si₂O₅-TiO₂, K₂O-TiO₂, Cs₂O-TiO₂ }</div>	880		11), 12)
		Ti-O stretching vibration of TiO ₅ square pyramid	
TiO ₂ -NaPO ₃ -Na ₂ B ₄ O ₇	930		13)
Na ₂ O-TiO ₂ -P ₂ O ₅	900		14)
<div>Ba₂TiSi₂O₈, Ba₂TiGe₂O₈ }</div>	830		15)
		Ti-O stretching vibration of TiO ₆ octahedra	
Na ₂ O-TiO ₂ -P ₂ O ₅	640		14)
TiO ₂ -NaPO ₃ -Na ₂ B ₄ O ₇	740		13)
K ₂ O-TiO ₂ , Cs ₂ O-TiO ₂	630-650		12)

sion on the medium-range-order are subjects in the future work. In addition, in the present work we neglected the effect of the Al^{3+} contaminant on the coordination state of P^{5+} and Ti^{4+} ions in the melt-derived glass. This was considered reasonable, by referring to the previous work on the $\text{R}_2\text{O}-\text{GeO}_2$ (R: alkali) glasses in which the addition of a small amount of Al_2O_3 did not bring about any essential change of the coordination state of Ge^{4+} ions.²⁴⁾ However, for more strict structure discussion, the structure analysis of the sol-gel-derived $\text{TiO}_2-\text{P}_2\text{O}_5$ glass added with a small amount of Al_2O_3 may be needed.

Summarizing the above-given structure data, it can be stated that the Ti^{4+} ion in higher coordination state is more abundant in the sol-gel-glass than in the melt-glass. The tendency of cations to prefer higher coordination state in the sol-gel-glass has been reported for Ge^{4+} ions in the $\text{Na}_2\text{O}-\text{GeO}_2$ glass system²⁵⁾ and Ti^{4+} ions in the $\text{Na}_2\text{O}-\text{TiO}_2$ glasses.²⁶⁾ From the view point of thermochemistry, this tendency is reasonable because higher coordination state of such cations is more stable at low temperatures and cations do not experience high temperatures during the sol-gel glass processing.

5. Conclusion

The structure of the sol-gel- and melt-derived $70\text{TiO}_2 \cdot 30\text{P}_2\text{O}_5$ (mol%) glasses was examined by means of FT-IR, Raman spectroscopy and X-ray diffraction method. Following results were obtained.

(1) FT-IR and Raman data revealed that Ti^{4+} ions are present in the 4 or 5, and 6-fold coordination states with respect to oxide ions. It was suggested that 6-fold coordinated Ti^{4+} ions are predominant in the sol-gel glass, while 4 and/or 5-fold Ti^{4+} ions coexist with a small amount of 6-fold ones in the melt-glass.

(2) From X-ray atomic radial distribution function curves, the coordination number of Ti^{4+} ions was evaluated to be almost 6 in the sol-gel glass, while 4–5 in the melt-glass. The coordination number of P^{5+} ions was 4 in both glasses.

(3) It was considered that PO_4 tetrahedra were interconnected mostly with TiO_6 octahedra in the sol-gel glass, and with TiO_4 and TiO_6 , or possibly with TiO_5 pyramidal units in the melt-glass.

References

- Vaughan, J. G., Perry, C. H. and Kinser, D. L., *Phys. Chem. Glasses*, Vol. 18, pp. 87–95 (1977).
- Hayashi, T. and Saito, H., *Phys. Chem. Glasses*, Vol. 20, pp. 108–114 (1979).
- Brow, R. K., Tallant, D. R., Warren, W. L., McIntyre, A. and Day, D. E., *Phys. Chem. Glasses*, Vol. 38, pp. 300–306 (1997).
- Hashimoto, T., Nijima, S., Nasu, H. and Kamiya, K., *J. Ceram. Soc. Japan*, Suppl., Vol. 112, S1193–S1199 (2004).
- Tang, A. J., Hashimoto, T., Nasu, H. and Kamiya, K., submitted, *Mater. Res. Bull.*
- Norman, N., *Acta Cryst.*, Vol. 10, pp. 370–372 (1957).
- Hoppe, U., Kranold, R., Stachel, D., Barz, A. and Hannon, A. C., *Z. Naturforsch A*, Vol. 55, pp. 369–380 (2000).
- Kusabiraki, K., *J. Non-Cryst. Solids*, Vol. 95 & 96, pp. 411–418 (1987).
- Morsi, M. M. and El-Shennam, A. W. A., *Phys. Chem. Glasses*, Vol. 25, pp. 64–68 (1984).
- Takahashi, K., Mochida, N. and Yoshida, Y., *J. Ceram. Soc. Japan (Yogyo-Kyokai-Shi)*, Vol. 85, pp. 26–36 (1977) [in Japanese].
- Furukawa, T. and White, W. B., *Phys. Chem. Glasses*, Vol. 20, pp. 69–80 (1979).
- Sakka, S., Miyaji, F. and Fukumi, K., *J. Non-Cryst. Solids*, Vol. 112, pp. 64–68 (1989).
- Cardinal, T., Fargin, E., Flem, G. L. and Couzi, M., *J. Solid State Chem.*, Vol. 120, pp. 151–156 (1995).
- Krimi, S., Jazouli, A. E., Rabardel, L., Couzi, M., Mansouri, J. and Flem, G. L., *J. Solid State Chem.*, Vol. 102, pp. 400–407 (1993).
- Markgraf, S. A., Sharma, S. K. and Bhalla, A. S., *J. Am. Ceram. Soc.*, Vol. 75, pp. 2630–2632 (1992).
- Wyckoff, R. W. G., "Crystal Structure," Interscience Publishers, New York, 3 (1968) pp. 447–448.
- Wyckoff, R. W. G., "Crystal Structure," Interscience Publishers, New York, 3 (1968) pp. 87–88.
- Wyckoff, R. W. G., "Crystal Structure," Interscience Publishers, New York, 3 (1968) pp. 444–445.
- Wyckoff, R. W. G., "Crystal Structure," Interscience Publishers, New York, 1 (1968) pp. 253–255.
- Wyckoff, R. W. G., "Crystal Structure," Interscience Publishers, New York, 3 (1968) pp. 101–102.
- Schartau, W. von and Hoppe, R., *Z. Anorg. Allg. Chem.*, Vol. 48, pp. 60–61 (1974).
- Wyckoff, R. W. G., "Crystal Structure," Interscience Publishers, New York, 3 (1968) pp. 312–313.
- Yarker, C. A., Johnson, P. A. V. and Wright, A. C., *J. Non-Cryst. Solids*, Vol. 79, pp. 117–136 (1986).
- Kamiya, K., Sakka, S. and Yoko, T., *Res. Rep. Fac. Eng. Mie Univ.*, Vol. 7, pp. 107–109 (1982).
- Kamiya, K., Tatsumi, M., Nasu, H. and Matsuoka, J., *J. Ceram. Soc. Japan*, Vol. 101, pp. 1201–1205 (1993).
- Harada, H., Kamiya, K., Nasu, H. and Matsuoka, J., *J. Sol-Gel Sci. Tech.*, Vol. 10, pp. 291–300 (1997).